

# Approximating committor functions: Objective functions and training data sampling

Thomas Pigeon

IFP Énergies nouvelles Lyon

*With T. Lelièvre (ENPC; INRIA) and G. Stoltz (ENPC, INRIA)*

Dimensionality reduction techniques for molecular dynamics  
2025, ICMS



## Modelled system

Chemical or biological systems are described as classical systems of  $N$  atoms with:

- Positions:  $\mathbf{q} \in \Omega$  where  $\Omega = \mathbb{R}^{3N}$  or  $(\mathbb{T}^3)^N$
- Momenta:  $\mathbf{p} \in \mathbb{R}^{3N}$
- Hamiltonian:  $H(\mathbf{q}, \mathbf{p}) = \frac{1}{2}\mathbf{p}^T M^{-1} \mathbf{p} + V(\mathbf{q})$

Evolution in time is modelled by underdamped Langevin dynamics (friction  $\gamma > 0$ )

$$\begin{cases} d\mathbf{q}_t = M^{-1} \mathbf{p}_t dt \\ d\mathbf{p}_t = -\nabla V(\mathbf{q}_t) dt - \gamma \mathbf{p}_t dt + \sqrt{\frac{2\gamma}{\beta}} M^{\frac{1}{2}} d\mathbf{W}_t. \end{cases} \quad (1)$$

such that positions and momenta are distributed according to Boltzmann–Gibbs measure:

$$\rho(d\mathbf{q}, d\mathbf{p}) = \frac{1}{Q} e^{-\beta H(\mathbf{q}, \mathbf{p})} d\mathbf{q} d\mathbf{p}. \quad (2)$$

The generator of this dynamics writes:

$$\mathcal{L}_{\text{und}} = -\nabla_{\mathbf{q}} V(\mathbf{q}) \cdot \nabla_{\mathbf{p}} + M^{-1} \mathbf{p} \cdot \nabla_{\mathbf{q}} - \gamma \mathbf{p} \cdot \nabla_{\mathbf{p}} + \frac{\gamma}{\beta} M : \nabla_{\mathbf{p}}^2. \quad (3)$$

## Modelled system

We can also consider the overdamped limit of the dynamics (1)  
 $(\gamma \rightarrow +\infty / M = m\text{Id}, m \rightarrow 0)$  :

$$d\mathbf{q}_t = -\nabla V(\mathbf{q}_t)dt + \sqrt{\frac{2}{\beta}}d\mathbf{W}t. \quad (4)$$

It is not adequate to describe the dynamics of most systems but its generator has a simpler expression than the one of underdamped dynamics:

$$\mathcal{L}_{\text{ovd}} = -\nabla V \cdot \nabla + \frac{1}{\beta}\Delta. \quad (5)$$

## Committer function

Chemical or biological processes are a succession of rare reactive  $A \rightarrow B$  events, where  $A, B \subset \Omega \times \mathbb{R}^{3N}$  such that  $A \cap B = \emptyset$ .

Most of the methodologies aiming at characterizing such reactive events require an importance function and for most of them the optimal one is the committor function:

$$p_{A \rightarrow B}(\mathbf{q}, \mathbf{p}) = \mathbb{P}^{\mathbf{q}, \mathbf{p}} [\tau_B < \tau_A]. \quad (6)$$

with  $\tau_X$  the first hitting time of the subset  $X$ .

Eventhough the overdamped dynamics is not adequate to describe dynamical behavior of the system, the associated committor function is already a good collective variable.

## Approximating committor function

The committor function being a high dimensional function, neural networks could be an efficient way of approximating it.

It boils down to identifying a minimization problem and the way to numerically solve it.

# Table of Contents

- 1 Some existing objective functions
- 2 Objective functions from Itō's formula
- 3 Comparison on the Müller–Brown Potential
- 4 Iterative learning with AMS

# Point-wise approximations and regression

Given the definition:

$$p_{A \rightarrow B}(\mathbf{q}) = \mathbb{P}^{\mathbf{q}} [\tau_B < \tau_A], \quad (7)$$

- select  $M$  configuration  $\mathbf{q}^i$
- for each  $\mathbf{q}^i$ , run  $L$  trajectories until either  $A$  or  $B$  is reached
- build the Monte-Carlo estimator  $\tilde{p}_{A \rightarrow B}(\mathbf{q}^i)$  for each  $\mathbf{q}$
- minimize  $\frac{1}{M} \sum_{i=1}^M (f(\mathbf{q}^i) - \tilde{p}_{A \rightarrow B}(\mathbf{q}^i))^2$

→ High variance of Monte-Carlo estimator when  $p_{A \rightarrow B}$  is close to 0 or 1, not efficient if the reaction is rare.

A similar approach is possible using transition path sampling (TPS) as this MCMC procedure requires to run two dynamics starting from a given point, then the committor can be estimated using negative log-likelihood loss.<sup>1</sup>.

→ Need initial path, still have the high variance close to  $A$  and  $B$ .

---

<sup>1</sup>Jung et al. [2023]

# Point-wise approximations and regression

Given an ensemble of "re-weighted" trajectories:<sup>2</sup>

- define some collective variables (CVs) in small dimension so that you can define a grid on it
- in each bins of the grid, count the number of trajectories going first in  $B$
- build the weighted estimator  $\tilde{p}_{A \rightarrow B}(\mathbf{q}^c)$  for each bin centers  $\mathbf{q}^c$
- minimize  $\sum_{c=1}^{N_{\text{bins}}} (f(\mathbf{q}^c) - \tilde{p}_{A \rightarrow B}(\mathbf{q}^c))^2$

→ Variance problem addressed by the re-weighting scheme

→ Need to define some some CVs that can parameterize the committor

→ Need to have CVs to run enhanced sampling methods to obtain the re-weighted path ensemble

→ Potential iterative approach scheme possible to address this problem

<sup>2</sup>Lopes and Lelièvre [2019]

## PDE residuals

The committor function verifies the PDE:

$$\begin{aligned} \forall \mathbf{q} \in \Omega \setminus (\overline{A} \cup \overline{B}), \quad \mathcal{L}_{\text{ovd}} p_{A \rightarrow B}(\mathbf{q}) &= 0, \\ \forall \mathbf{q} \in \overline{A}, \quad p_{A \rightarrow B}(\mathbf{q}) &= 0, \quad \forall \mathbf{q} \in \overline{B}, \quad p_{A \rightarrow B}(\mathbf{q}) = 1, \end{aligned} \tag{8}$$

with  $\overline{A} = A \cup \partial A$ ,  $\overline{B} = B \cup \partial B$  and:

$$\mathcal{L}_{\text{ovd}} = -\nabla V \cdot \nabla + \frac{1}{\beta} \Delta.$$

Following the PINN approach,<sup>3</sup> the committor can be approximated by considering the minimization problem:

$$\operatorname{arginf}_f \left\{ \int_{\Omega \setminus (\overline{A} \cup \overline{B})} |\mathcal{L}_{\text{ovd}} f(\mathbf{q})|^2 \mu(d\mathbf{q}) \mid f(\mathbf{q}) = 0, \mathbf{q} \in \overline{A}, \quad f(\mathbf{q}) = 1, \mathbf{q} \in \overline{B} \right\}. \tag{9}$$

---

<sup>3</sup>Raissi et al. [2017]

# PDE residuals

$$\operatorname{arginf}_f \left\{ \int_{\Omega \setminus (\bar{A} \cup \bar{B})} |\mathcal{L}_{\text{ovd}} f(\mathbf{q})|^2 \mu(d\mathbf{q}) \mid f(\mathbf{q}) = 0, \mathbf{q} \in \bar{A}, f(\mathbf{q}) = 1, \mathbf{q} \in \bar{B} \right\}.$$

There are two ways to address the boundary conditions problem.<sup>4</sup>

- functional form :  $f(\mathbf{q}) = \tilde{\mathbb{1}}_{(A \cup B)^c}(\mathbf{q}) p_\theta(\mathbf{q}) + \tilde{\mathbb{1}}_{A \cup B}(\mathbf{q}) \tilde{\mathbb{1}}_B(\mathbf{q})$  where  $\tilde{\mathbb{1}}_X$  is the continuous function infinitely close to the indicator function of state  $X$ .<sup>5</sup>
- penalization term :  $\alpha \left( \int_{\bar{A}} (f(\mathbf{q}))^2 d\mathbf{q} + \int_{\bar{B}} (f(\mathbf{q}) - 1)^2 d\mathbf{q} \right)$  where  $\alpha \rightarrow +\infty$ .

→  $\mu$  can be an arbitrary distribution as far as it has full support on  $\Omega \setminus (\bar{A} \cup \bar{B})$   
→ Need to compute 2<sup>nd</sup> order derivatives with respect to input

<sup>4</sup> Barschkis [2023]

<sup>5</sup> Li et al. [2019]

## PDE variational formulation

The committor is the solution of the minimization problem:

$$\operatorname{arginf}_f \left\{ \int_{\Omega \setminus (\bar{A} \cup \bar{B})} |\nabla f(\mathbf{q})|^2 e^{-\beta V(\mathbf{q})} d\mathbf{q} \middle| f(\mathbf{q}) = 0, \mathbf{q} \in \bar{A}, f(\mathbf{q}) = 1, \mathbf{q} \in \bar{B}. \right\}, \quad (10)$$

as the critical points of this functional satisfy the PDE (8).<sup>6</sup>

- Need a sample of Boltzmann-Gibbs measure restricted to  $\Omega \setminus (\bar{A} \cup \bar{B})$
- Iterative enhanced-sampling and training procedure can address this problem<sup>7</sup>

---

<sup>6</sup>Khoo et al. [2018], Li et al. [2019]

<sup>7</sup>Rotskoff and Vanden-Eijnden [2020], Rotskoff et al. [2022], Yuan et al. [2023], Kang et al. [2024], Wang et al. [2025] ↗

## Fixed point reformulation

Given  $\tau := \min(\tau_A, \tau_B)$ , the committor is a fixed point of the operator<sup>8</sup>

$$(\mathcal{P}_t f)(\mathbf{q}_0) = \mathbb{E}^{\mathbf{q}_0} [f(\mathbf{q}_{t \wedge \tau})]$$

so that:

$$\forall t \geq 0, \forall \mathbf{q} \in \Omega \setminus (\overline{A} \cup \overline{B}), \quad p_{A \rightarrow B}(\mathbf{q}) = (\mathcal{P}_t p_{A \rightarrow B})(\mathbf{q}). \quad (11)$$

We also introduce the notation:

$$\begin{aligned} (\mathcal{P}_t f)(\mathbf{q}_0) &= \mathbb{E}^{\mathbf{q}_0} [f(\mathbf{q}_t) \mathbb{1}_{t < \tau}] + \mathbb{E}^{\mathbf{q}_0} [f(\mathbf{q}_\tau) \mathbb{1}_{t \geq \tau}] \\ &= (\mathcal{P}_t^i f)(\mathbf{q}_0) + (\mathcal{P}_t^b f)(\mathbf{q}_0), \end{aligned} \quad (12)$$

so that we can write:

$$\forall t > 0, \forall \mathbf{q} \in \Omega \setminus (\overline{A} \cup \overline{B}), \quad (\text{Id} - \mathcal{P}_t^i) p_{A \rightarrow B}(\mathbf{q}) - (\mathcal{P}_t^b \mathbb{1}_B)(\mathbf{q}) = 0, \quad (13)$$

and  $p_{A \rightarrow B}$  is the only solution of:

$$f = \mathcal{P}_t^i f + \mathcal{P}_t^b \mathbb{1}_B \quad (14)$$

---

<sup>8</sup>Li et al. [2022]

## Fixed point residuals

The committor is the solution to the minimization problem:<sup>9</sup>

$$\operatorname{arginf}_f \left\{ \int_{\Omega \setminus (\bar{A} \cup \bar{B})} \left[ (\text{Id} - \mathcal{P}_t^i) f(\mathbf{q}) - (\mathcal{P}_t^b \mathbb{1}_B)(\mathbf{q}) \right]^2 \mu(d\mathbf{q}) \right\}. \quad (15)$$

With:

$$\varphi(\mathbf{q}_0, \mathbf{q}_t) = f(\mathbf{q}_0) - f(\mathbf{q}_t) \mathbb{1}_{t < \tau} - \mathbb{1}_P(\mathbf{q}_t) \mathbb{1}_{t \geq \tau},$$

so that:

$$(\text{Id} - \mathcal{P}_t^i) f(\mathbf{q}) - (\mathcal{P}_t^b \mathbb{1}_B)(\mathbf{q}) = \mathbb{E} [\varphi(\mathbf{q}_0, \mathbf{q}_t)].$$

(15) rewrites:

$$\operatorname{arginf}_f \left\{ \mathbb{E}_\mu \left[ \mathbb{E} [\varphi(\mathbf{q}_0, \mathbf{q}_t)]^2 \right] \right\},$$

→  $\mu$  can be arbitrary as far as it has full support on  $\Omega \setminus (\bar{A} \cup \bar{B})$

→ The boundary conditions are directly included in the problem

<sup>9</sup>Strahan et al. [2023]

## Fixed point residuals

Assuming we can draw independently  $n$  configuration  $\mathbf{q}_0^i$  from  $\mu$  and for each of them we run independently two dynamics:

$$\lim_{n \rightarrow +\infty} \frac{1}{n} \sum_{i=1}^n \varphi(\mathbf{q}_0^i, \mathbf{q}_t^{i,1}) \varphi(\mathbf{q}_0^i, \mathbf{q}_t^{i,2}) = \mathbb{E}^\mu \left[ \mathbb{E} [\varphi(\mathbf{q}_0, \mathbf{q}_t) | \mathbf{q}_0 = \mathbf{q}]^2 \right].$$

→ At least two trajectories must be used to estimate the loss numerically

## Fixed point residuals

As the committor function can be extremely close to 0 (resp. 1) in the vicinity of  $A$  (reps.  $B$ ), it was proposed to apply the log to (14):<sup>10</sup>

$$\operatorname{arginf}_f \left\{ \int_{\Omega \setminus (\bar{A} \cup \bar{B})} [\ln(f(\mathbf{q})) - \ln(\mathcal{P}_t^i f(\mathbf{q}) + \mathcal{P}_t^b \mathbb{1}_B(\mathbf{q}))]^2 \mu(d\mathbf{q}) \right\}. \quad (16)$$

Due to Jensen's inequality, the empirical estimator of this functional is biased but the authors argues that this has a minor effect and the benefit of using the log is stronger.

---

<sup>10</sup> Mitchell and Rotskoff [2024]

## Fixed point variational formulation

The committor function is the solution to the minimization problem:<sup>11</sup>

$$\operatorname{arginf}_f \left\{ \int_{\Omega \setminus (\bar{A} \cup \bar{B})} f(\mathbf{q}) \left[ (\text{Id} - \mathcal{P}_t^i) f(\mathbf{q}) - 2\mathcal{P}_t^b \mathbb{1}_B(\mathbf{q}) \right] e^{-\beta V(\mathbf{q})} d\mathbf{q} \right\}. \quad (17)$$

The same approach was used in<sup>12</sup> but reformulating this as:

$$\operatorname{arginf}_f \left\{ \int_{\Omega} (\mathcal{P}_t f(\mathbf{q})^2 - 2f(\mathbf{q})\mathcal{P}_t f(\mathbf{q}) + f(\mathbf{q})) e^{-\beta V(\mathbf{q})} d\mathbf{q} \middle| f(\mathbf{q}) = 0, \mathbf{q} \in \bar{A}, f(\mathbf{q}) = 1, \mathbf{q} \in \bar{B} \right\}. \quad (18)$$

---

<sup>11</sup>Li et al. [2019]

<sup>12</sup>Roux [2021], He et al. [2022], Roux [2022], Chen et al. [2023]

# Summary of existing methods

Estimation and regression methods:

→ Need enhanced sampling to get accurate estimations close to  $A$  and  $B$

Other approaches:

	PDE $\mathcal{L}_{\text{ovd}}$	Fixed point $\mathcal{P}_t$
Residuals	1, 2	1, 3, 4
Variational	5, 6	5, 6

- 1. Any measure  $\mu$  with full support on  $\Omega \setminus (\bar{A} \cup \bar{B})$
- 2. Need to compute second order derivatives
- 3. Need multiple trajectories for each configurations in the sample of  $\mu$
- 4. Can use ln function to improve the accuracy close to  $A$  and  $B$
- 5. Need sample of Boltzman-Gibbs measure restricted to  $\Omega \setminus (\bar{A} \cup \bar{B})$
- 6. Limited to overdamped dynamics

# Table of Contents

- 1 Some existing objective functions
- 2 Objective functions from Itō's formula
- 3 Comparison on the Müller–Brown Potential
- 4 Iterative learning with AMS

## Function of the scaled and shifted committor

Let's consider  $h \in C^2(I)$ , where  $I$  is an interval of  $\mathbb{R}$  and two real numbers  $(a, b)$  such that  $(\min(a + b, b), \max(a + b, b)) \subset I$ ,

$$\begin{aligned}\mathcal{L}_{\text{ovd}} h(a p_{A \rightarrow B}(\mathbf{q}) + b) \\ &= -\nabla V(\mathbf{q}) \cdot \nabla [h(a p_{A \rightarrow B}(\mathbf{q}) + b)] + \frac{1}{\beta} \Delta [h(a p_{A \rightarrow B}(\mathbf{q}) + b)] \\ &= -a h'(a p_{A \rightarrow B}(\mathbf{q}) + b) \nabla V(\mathbf{q}) \cdot \nabla p_{A \rightarrow B}(\mathbf{q}) \\ &\quad + \frac{1}{\beta} \nabla \cdot [a h'(a p_{A \rightarrow B}(\mathbf{q}) + b) \nabla p_{A \rightarrow B}(\mathbf{q})] \\ &= -a h'(a p_{A \rightarrow B}(\mathbf{q}) + b) \mathcal{L}_{\text{ovd}} p_{A \rightarrow B}(\mathbf{q}) + \frac{a^2}{\beta} h''(a p_{A \rightarrow B}(\mathbf{q}) + b) |\nabla p_{A \rightarrow B}(\mathbf{q})|^2,\end{aligned}$$

Given the backward Kolmogorov equation (8), we finally obtain:

$$\mathcal{L}_{\text{ovd}} h(a p_{A \rightarrow B}(\mathbf{q}) + b) = \frac{a^2}{\beta} h''(a p_{A \rightarrow B}(\mathbf{q}) + b) |\nabla p_{A \rightarrow B}(\mathbf{q})|^2. \quad (19)$$

## Itō's lemma

The Itō's formula leads to:

$$\begin{aligned} dh(a p_{A \rightarrow B}(\mathbf{q}_t) + b) &= \frac{a^2}{\beta} h''(a p_{A \rightarrow B}(\mathbf{q}_t) + b) |\nabla p_{A \rightarrow B}(\mathbf{q}_t)|^2 dt \\ &\quad + \sqrt{\frac{2}{\beta}} a h'(a p_{A \rightarrow B}(\mathbf{q}_t) + b) \nabla p_{A \rightarrow B}(\mathbf{q}_t) \cdot d\mathbf{W}_t. \end{aligned}$$

By integrating until time  $t \wedge \tau$ , for any  $\mathbf{q}_0 \in \Omega \setminus (\overline{R} \cup \overline{P})$ , we then obtain:

$$\begin{aligned} &h(a p_{A \rightarrow B}(\mathbf{q}_t) + b) \mathbb{1}_{t < \tau} + h(a \mathbb{1}_B(\mathbf{q}_\tau) + b) \mathbb{1}_{t \geq \tau} - h(a p_{A \rightarrow B}(\mathbf{q}_0) + b) \\ &= \frac{a^2}{\beta} \int_0^{t \wedge \tau} h''(a p_{A \rightarrow B}(\mathbf{q}_s) + b) |\nabla p_{A \rightarrow B}(\mathbf{q}_s)|^2 ds \\ &\quad + a \sqrt{\frac{2}{\beta}} \int_0^{t \wedge \tau} h'(a p_{A \rightarrow B}(\mathbf{q}_s) + b) \nabla p_{A \rightarrow B}(\mathbf{q}_s) \cdot d\mathbf{W}_s. \end{aligned}$$

## Alternative loss

New objective:

$$\operatorname{arginf}_f \int_{\Omega \setminus (\bar{A} \cup \bar{B})} \left( h(a f(\mathbf{q}_t) + b) \mathbb{1}_{t < \tau} + h(a \mathbb{1}_B(\mathbf{q}_\tau) + b) \mathbb{1}_{t \geq \tau} - h(a f(\mathbf{q}_0) + b) \right. \\ \left. - \frac{a^2}{\beta} \int_0^{t \wedge \tau} h''(a f(\mathbf{q}_s) + b) |\nabla f(\mathbf{q}_s)|^2 ds \right. \\ \left. - a \sqrt{\frac{2}{\beta}} \int_0^{t \wedge \tau} h'(a f(\mathbf{q}_s) + b) \nabla f(\mathbf{q}_s) \cdot d\mathbf{W}_s \right)^2 \mu(d\mathbf{q}_0), \quad (20)$$

## Extension to biased dynamics

Let's consider the biased dynamics:

$$d\mathbf{q}_t = -\nabla_q(V - U)(\mathbf{q}_t)dt + \sqrt{\frac{2}{\beta}}d\mathbf{W}_t. \quad (21)$$

The corresponding infinitesimal generator writes:

$$\mathcal{L}_U = -\nabla_q(V - U) \cdot \nabla_q + \frac{1}{\beta} \Delta_q = \mathcal{L}_{\text{ovd}} + \nabla_q U \cdot \nabla_q, \quad (22)$$

so that its action on a function of the scaled and shifted committor function writes:

$$\begin{aligned} \mathcal{L}_U h(a p_{A \rightarrow B}(\mathbf{q}) + b) &= \mathcal{L}_{\text{ovd}} h(a p_{A \rightarrow B}(\mathbf{q}) + b) \\ &\quad + ah' (a p_{A \rightarrow B}(\mathbf{q}) + b) \nabla p_{A \rightarrow B}(\mathbf{q}) \cdot \nabla U(\mathbf{q}). \end{aligned} \quad (23)$$

## Extension to biased dynamics

Applying Itō's formula considering the stochastic process (21), we obtain:

$$\begin{aligned} d[h(a p_{A \rightarrow B}(\mathbf{q}_t) + b)] &= \frac{a^2}{\beta} h''(a p_{A \rightarrow B}(\mathbf{q}_t) + b) |\nabla p_{A \rightarrow B}(\mathbf{q}_t)|^2 dt \\ &\quad + a h'(a p_{A \rightarrow B}(\mathbf{q}_t) + b) \nabla p_{A \rightarrow B}(\mathbf{q}_t) \cdot \left( \sqrt{\frac{2}{\beta}} d\mathbf{W}_t + \nabla U(\mathbf{q}_t) dt \right), \end{aligned} \tag{24}$$

which lead to the minimization problem:

$$\begin{aligned} \operatorname{arginf}_f \int_{\Omega \setminus (\bar{A} \cup \bar{B})} & \left( h(a f(\mathbf{q}_t) + b) \mathbb{1}_{t < \tau} + h(a \mathbb{1}_B(\mathbf{q}_t) + b) \mathbb{1}_{t \geq \tau} - h(a f(\mathbf{q}_0) + b) \right. \\ & - \frac{a^2}{\beta} \int_0^{t \wedge \tau} h''(a f(\mathbf{q}_s) + b) |\nabla f(\mathbf{q}_s)|^2 ds \\ & - a \int_0^{t \wedge \tau} h'(a f(\mathbf{q}_s) + b) \nabla f(\mathbf{q}_s) \cdot \nabla U(\mathbf{q}_s) ds \\ & \left. - a \sqrt{\frac{2}{\beta}} \int_0^{t \wedge \tau} h'(a f(\mathbf{q}_s) + b) \nabla f(\mathbf{q}_s) \cdot d\mathbf{W}_s \right)^2 \mu(d\mathbf{q}_0), \end{aligned} \tag{25}$$

## Discretized loss

We use the parameterized committor:<sup>13</sup>

$$f_\theta(\mathbf{q}) = \tilde{\mathbb{1}}_{(R \cup P)^c}(\mathbf{q}) p_\theta(\mathbf{q}) + \tilde{\mathbb{1}}_{R \cup P}(\mathbf{q}) \tilde{\mathbb{1}}_P(\mathbf{q}), \quad (26)$$

where  $p_\theta$  is the (smooth) NN and  $\tilde{\mathbb{1}}$  are smooth indicator functions that are non zero extremely close to the set.

Consider the Euler-Maruyama integration scheme:

$$\mathbf{q}^{\ell+1} = \mathbf{q}^\ell - \nabla(V - U)(\mathbf{q}^\ell) \Delta t + \sqrt{\frac{2\Delta t}{\beta}} \mathbf{G}^{\ell+1}. \quad (27)$$

---

<sup>13</sup>Li et al. [2019]

## Discretized loss

Then we draw  $K$  configurations from the measure  $\mu$  and for each of them integrate the dynamics independently for  $L$  integration time steps  $\Delta t$ .

We define  $l_k$  as the smallest integer such that  $\mathbf{q}^{k,l_k} \in \overline{A} \cup \overline{B}$ ,  
using the notation  $T_k = L \wedge l_k$  the discretized loss writes:

$$\begin{aligned} & \frac{1}{K} \sum_{k=1}^K \left( h(a f_\theta(\mathbf{q}^{k,T_k}) + b) - h(a f_\theta(\mathbf{q}^{k,0}) + b) \right. \\ & \quad \left. - \frac{a^2 \Delta t}{\beta} \sum_{\ell=1}^{T_k} h''(a f_\theta(\mathbf{q}^{k,\ell}) + b) |\nabla f_\theta(\mathbf{q}^{k,\ell})|^2 \right. \\ & \quad \left. - a \sum_{\ell=1}^{T_k} h'(a f_\theta(\mathbf{q}^{k,\ell}) + b) \nabla f_\theta(\mathbf{q}^{k,\ell}) \cdot \left( \sqrt{\frac{2 \Delta t}{\beta}} \mathbf{G}^{k,\ell+1} + \nabla U(\mathbf{q}^{k,\ell}) \Delta t \right) \right)^2. \end{aligned} \tag{28}$$

## Choice of function $h$

$$\begin{aligned} & \frac{1}{K} \sum_{k=1}^K \left( h(\mathbf{a} f_\theta(\mathbf{q}^{k,T_k}) + \mathbf{b}) - h(\mathbf{a} f_\theta(\mathbf{q}^{k,0}) + \mathbf{b}) \right. \\ & \quad \left. - \frac{\mathbf{a}^2 \Delta t}{\beta} \sum_{\ell=1}^{T_k} h''(\mathbf{a} f_\theta(\mathbf{q}^{k,\ell}) + \mathbf{b}) |\nabla f_\theta(\mathbf{q}^{k,\ell})|^2 \right. \\ & \quad \left. - \mathbf{a} \sum_{\ell=1}^{T_k} h'(\mathbf{a} f_\theta(\mathbf{q}^{k,\ell}) + \mathbf{b}) \nabla f_\theta(\mathbf{q}^{k,\ell}) \cdot \left( \sqrt{\frac{2 \Delta t}{\beta}} \mathbf{G}^{k,\ell+1} + \nabla U(\mathbf{q}^{k,\ell}) \right) \right)^2. \end{aligned}$$

- $h = \text{Id}$ , then  $\mathbf{a} = 1$  and  $\mathbf{b} = 0$
- $h = \ln$ , sum of two losses (28),
  - ▶ 1<sup>st</sup> with  $\mathbf{a} = 1$  and  $\mathbf{b} = \varepsilon$
  - ▶ 2<sup>nd</sup> with  $\mathbf{a} = -1$  and  $\mathbf{b} = 1 + \varepsilon$

$\varepsilon \in (0, 1)$  introduced to prevent numerical issues and to introduce progressively the logarithm function.

# Table of Contents

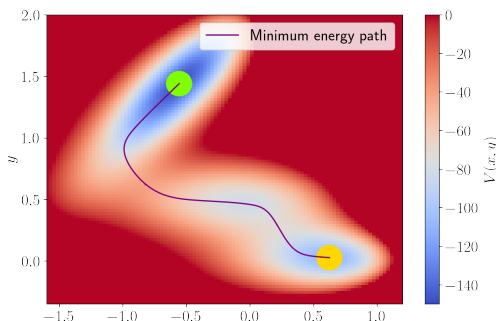
- 1 Some existing objective functions
- 2 Objective functions from Itō's formula
- 3 Comparison on the Müller–Brown Potential
- 4 Iterative learning with AMS

## Potential and states definitions

The 2D Müller–Brown potential<sup>14</sup> writes:

$$V(x_1, x_2) = \sum_{i=1}^4 A_i \exp \left( a_i (x_1 - u_i)^2 + b_i (x_1 - u_i)(x_2 - v_i) + c_i (x_2 - v_i)^2 \right), \quad (29)$$

with the parameters  $A = (-200, -100, -170, 15)$ ,  $a = (-1, -1, -6.5, 0.7)$ ,  $b = (0, 0, 11, 0.6)$ ,  $c = (-10, -10, -6.5, 0.7)$ ,  $u = (1, 0, -0.5, -1)$  and  $v = (0, 0.5, 1.5, 1)$ .



Unbiased overdamped dynamics with  $\beta = 0.05$  and  $\Delta t = 10^{-4}$

$A$  and  $B$  are small discs of radii 0.1 centered respectively at  $(-0.558, 1.442)$  and  $(0.623, 0.028)$

# Neural network training parameters and error metrics

Neural network training:

- Fully connected feed-forward NN with 2 hidden layers of 20 neurons with Tanh activation function and sigmoid output
- Adam optimizer with 0.001 fixed learning rate
- Training stopped after 50 epochs without decrease of validation loss
- $\frac{1}{4}$  training,  $\frac{1}{4}$  validation,  $\frac{1}{2}$  test

Error of the trained model computed against finite element approximation of committor.

- RMSE-r: RMSE of committor function computed on a set of points distributed according to reactive trajectories measure
- RMSE-log-b: RMSE of the log of committor computed on a set of points distributed according to Boltzmann–Gibbs measure

## With Boltzmann–Gibbs distribution

We obtain a sample of Boltzmann–Gibbs measure restricted to  $\Omega \setminus (\overline{A} \cup \overline{B})$  by integrating (27) for  $2 \times 10^5$  time-steps.

From this trajectory, we build various datasets composed of  $3.2 \times 10^4$  configurations to minimize (10), (17), (18) and (28).

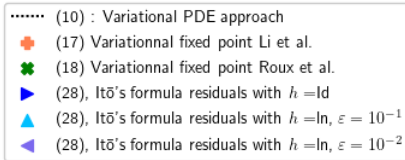
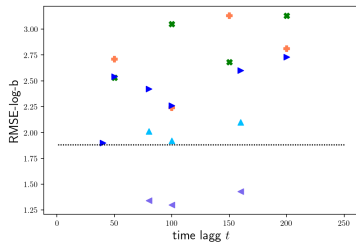
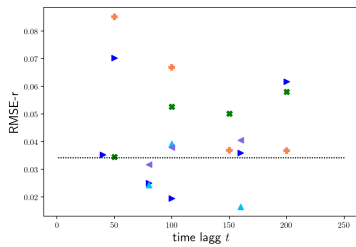
The batch size was fixed to 100 for the first 3 cases and fixed to 10 for the loss based on Itô's formula.

To be able to compare these methods, we initialize 10 NN and each of them is trained until early stopping 10 times, changing the random number seed for the mini-batching procedure.

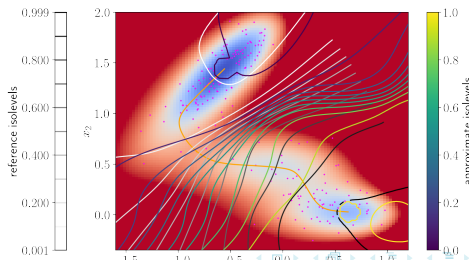
We present errors of the model with the lowest test loss.

# With Boltzmann–Gibbs distribution

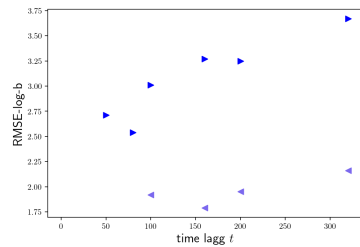
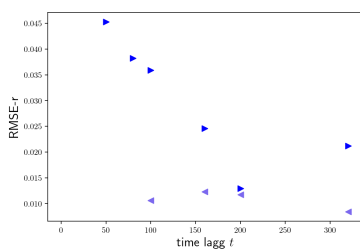
Dataset of  $3.2 \cdot 10^4$  configurations



Isolevels of a model with:  
 $\text{RMSE-r} = 0.025$  and  $\text{RMSE-long-b} = 1.62$



# With uniform distribution



Dataset of  $3.2 \cdot 10^5$  configurations

- (28), Itō's formula residuals with  $h = \text{Id}$
- (28), Itō's formula residuals with  $h = \ln, \varepsilon = 10^{-2}$

Isolevels of a model with:  
 $\text{RMSE-r} = 0.018$  and  $\text{RMSE-log-b} = 1.65$

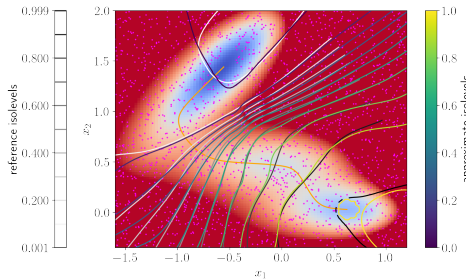


# Table of Contents

- 1 Some existing objective functions
- 2 Objective functions from Itō's formula
- 3 Comparison on the Müller–Brown Potential
- 4 Iterative learning with AMS

## Description of the procedure

- ① Define states  $A$  and  $B$  sample initial conditions for AMS<sup>15</sup> (exits of  $A$  and  $B$ ) with unbiased MD
- ② Cut trajectories in a dataset of sub-trajectories of fixed length  $L$  and train a first committor approximation
- ③ Run AMS to sample reactive trajectories. Re-weight the trajectories<sup>16</sup> and cut them in sub trajectories of length  $L$
- ④ Retrain the NN with extended dataset
- ⑤ Run AMS again. Measure the impact of extending the dataset, if no impact, stop the procedure, got back to 3 otherwise

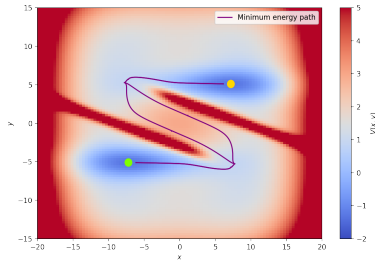
---

<sup>15</sup>Cérou and Guyader [2007], Lopes and Lelièvre [2019]

<sup>16</sup>Bréhier et al. [2015]

# Potential and state definition

Illustration on the Z-potential:<sup>17</sup>



Unbiased overdamped dynamics with  
 $\beta = 3$  and  $\Delta t = 0.05$

$A$  and  $B$  are small discs of radii 0.5  
centered respectively at  $(-7.20, -5.10)$   
and  $(7.20, 5.10)$

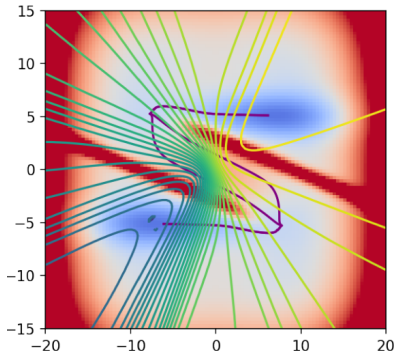
Way to measure the impact of increasing the dataset: linear regression between the log of the approximate committor values before and after extending the dataset.

We use a set of 1000 configurations randomly chosen within the reactive trajectories distribution.

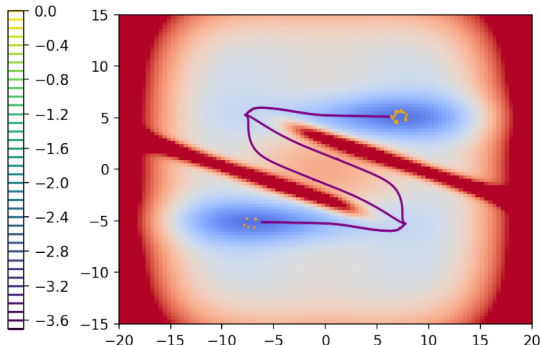
<sup>17</sup>Frassek et al. [2021]

# Iterative procedure results

First training before AMS with trajectories only near  $A$  and  $B$ :



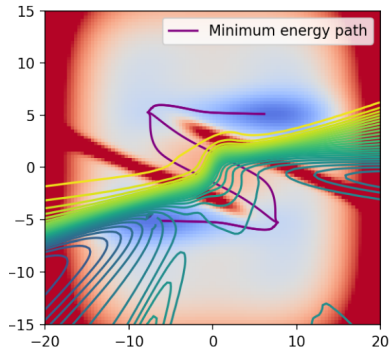
Isolevels of the log of the NN committor approximation



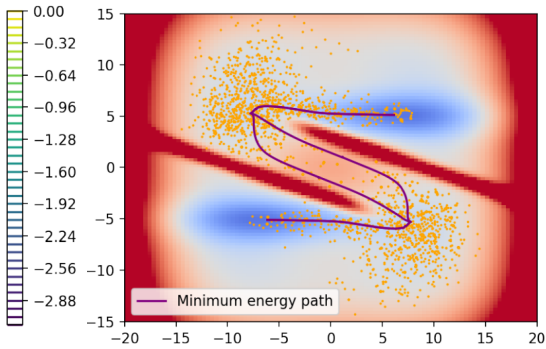
Initial configurations of sub-trajectories in the training dataset

# Iterative procedure results

Second training after first AMS:



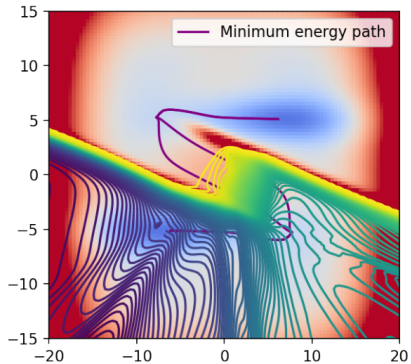
Isolevels of the log of the NN committor approximation



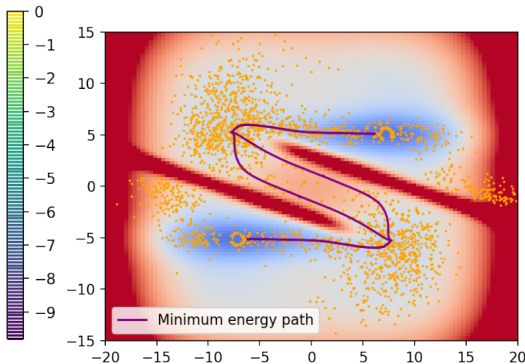
Initial configurations of sub-trajectories in the training dataset

# Iterative procedure results

Third training after second AMS:



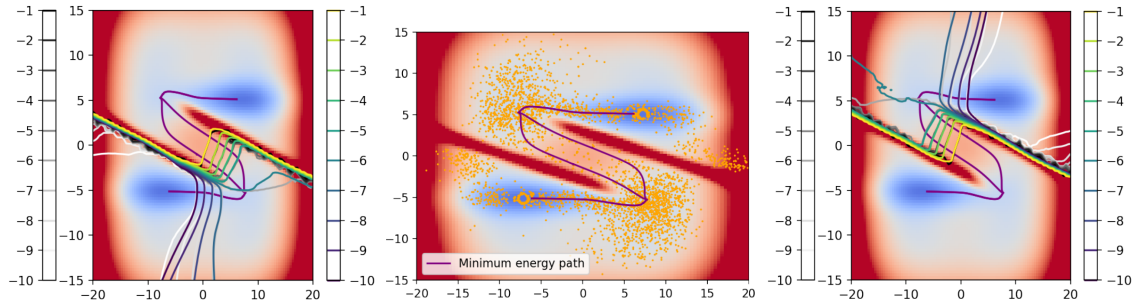
Isolevels of the log of the NN committor approximation



Initial configurations of sub-trajectories in the training dataset

# Iterative procedure results

Final model at the end of the procedure, comparison to finite elements approximation



## Comparison of reaction coordinates

95% confidence interval of the transition probability estimated with 100 forward and backward AMS runs using various reaction coordinates.

RC	$\xi_{\text{interp}}$	NN committor	FE committor
$A \rightarrow B$ $p \pm \frac{1.96}{\sqrt{10}} \sigma_p$	$(3.39 \pm 6.58) \times 10^{-8}$	$(4.41 \pm 1.07) \times 10^{-7}$	$(5.58 \pm 1.02) \times 10^{-7}$
$B \rightarrow A$ $p \pm \frac{1.96}{\sqrt{10}} \sigma_p$	$(0.89 \pm 1.52) \times 10^{-8}$	$(6.57 \pm 1.48) \times 10^{-7}$	$(5.09 \pm 1.) \times 10^{-7}$

$$\xi_{\text{interp}}(x, y) = (x_B - x_A) x + (y_B - y_A) y$$

## Conclusion & perspectives

This method allows to define satisfying reaction coordinate for AMS (in the sense of AMS variance)

Extend to underdamped dynamics and real systems.

Thank you!

## Variational loss

$$\operatorname{arginf}_f \left\{ \int_{\Omega \setminus (\bar{A} \cup \bar{B})} |\nabla f(\mathbf{q})|^2 e^{-\beta V(\mathbf{q})} d\mathbf{q}, \left| \begin{array}{l} f(\mathbf{q}) = 0, \mathbf{q} \in \bar{A}, \\ f(\mathbf{q}) = 1, \mathbf{q} \in \bar{B}. \end{array} \right. \right\}$$

$f_\lambda(\mathbf{q}) = p^*(\mathbf{q}) + \lambda \eta(\mathbf{q})$  where  $p^*$  is a critical point of the minimized functional.

$$\begin{aligned} 0 &= \frac{1}{2} \frac{\partial}{\partial \lambda} \int_{\Omega \setminus (\bar{A} \cup \bar{B})} |\nabla f_\lambda(\mathbf{q})|^2 e^{-\beta V(\mathbf{q})} d\mathbf{q} \Big|_{\lambda=0} \\ &= \int_{\Omega \setminus (\bar{A} \cup \bar{B})} \nabla \eta(\mathbf{q}) \cdot \nabla p^*(\mathbf{q}) e^{-\beta V(\mathbf{q})} d\mathbf{q} \\ &= \int_{\Omega \setminus (\bar{A} \cup \bar{B})} \nabla \cdot (\eta(\mathbf{q}) \nabla p^*(\mathbf{q}) e^{-\beta V(\mathbf{q})}) d\mathbf{q} \\ &\quad - \int_{\Omega \setminus (R \cup P)} \eta(\mathbf{q}) \nabla \cdot (\nabla p^*(\mathbf{q}) e^{-\beta V(\mathbf{q})}) d\mathbf{q}. \end{aligned}$$

## Variational PDE loss

Since for all functions  $\eta$  such that  $\forall \mathbf{q} \in (\partial R \cup \partial P), \eta(\mathbf{q}) = 0$

$$\int_{\Omega \setminus (\bar{A} \cup \bar{B})} \nabla \cdot \left( \eta(\mathbf{q}) \nabla p^*(\mathbf{q}) e^{-\beta V(\mathbf{q})} \right) d\mathbf{q} = \int_{\partial(\Omega \setminus (\bar{A} \cup \bar{B}))} \eta(\mathbf{q}) \nabla p^*(\mathbf{q}) e^{-\beta V(\mathbf{q})} ds = 0,$$

We have

$$0 = - \int_{\Omega \setminus (\bar{A} \cup \bar{B})} \eta(\mathbf{q}) \nabla \cdot \left( \nabla p^*(\mathbf{q}) e^{-\beta V(\mathbf{q})} \right) d\mathbf{q}.$$

$$0 = - \int_{\Omega \setminus (\bar{A} \cup \bar{B})} \eta(\mathbf{q}) (\Delta p^*(\mathbf{q}) - \beta \nabla p^*(\mathbf{q}) \cdot \nabla V(\mathbf{q})) e^{-\beta V(\mathbf{q})} d\mathbf{q}$$

$$0 = - \int_{\Omega \setminus (\bar{A} \cup \bar{B})} \eta(\mathbf{q}) \beta (\mathcal{L}_{\text{ovd}} p^*)(\mathbf{q}) e^{-\beta V(\mathbf{q})} d\mathbf{q},$$

## Fixed point justification

$\forall \mathbf{q}_0 \in \Omega \setminus (\overline{A} \cup \overline{B}),$

$$p_{A \rightarrow B}(\mathbf{q}_t) \mathbb{1}_{t < \tau_{\overline{A} \cup \overline{B}}} + \mathbb{1}_{\overline{B}}(\mathbf{q}_{\tau_{\overline{A} \cup \overline{B}}}) \mathbb{1}_{t \geq \tau_{\overline{A} \cup \overline{B}}} - p_{A \rightarrow B}(\mathbf{q}_0) = \int_0^{t \wedge \tau_{\overline{A} \cup \overline{B}}} \sqrt{\frac{2}{\beta}} \nabla p_{A \rightarrow B}(\mathbf{q}_s) \cdot d\mathbf{W}_s$$

Taking the expectation with respect to the law of the process we get:

$$\forall \mathbf{q} \in \Omega \setminus (\overline{A} \cup \overline{B}), (\mathcal{P}^i - I)p_{A \rightarrow B}(\mathbf{q}) + \mathcal{P}^b \mathbb{1}_{\overline{B}}(\mathbf{q}) = 0.$$

## Variational fixed point loss

$$\operatorname{arginf}_f \left\{ \frac{1}{2} \int_{\Omega \setminus (\bar{A} \cup \bar{B})} f(\mathbf{q}) (I - \mathcal{P}^i) f(\mathbf{q}) e^{-\beta V(\mathbf{q})} d\mathbf{q} - \int_{\Omega \setminus (\bar{A} \cup \bar{B})} f(\mathbf{q}) \mathcal{P}^b 1_{\bar{B}}(\mathbf{q}) e^{-\beta V(\mathbf{q})} d\mathbf{q} \right\}$$

$$f_\lambda(\mathbf{q}) = p^*(\mathbf{q}) + \lambda \eta(\mathbf{q}),$$

$$\begin{aligned} 0 &= \frac{\partial}{\partial \lambda} \left( \frac{1}{2} \int_{\Omega \setminus (\bar{A} \cup \bar{B})} f_\lambda(\mathbf{q}) (I - \mathcal{P}^i) f_\lambda(\mathbf{q}, \lambda) e^{-\beta V(\mathbf{q})} d\mathbf{q} \right. \\ &\quad \left. - \int_{\Omega \setminus (\bar{A} \cup \bar{B})} f_\lambda(\mathbf{q}, \lambda) \mathcal{P}^b 1_{\bar{B}}(\mathbf{q}) e^{-\beta V(\mathbf{q})} d\mathbf{q} \right) \Big|_{\lambda=0} \\ &= \int_{\Omega \setminus (\bar{A} \cup \bar{B})} \eta(\mathbf{q}) (I - \mathcal{P}^i) p^*(\mathbf{q}) e^{-\beta V(\mathbf{q})} d\mathbf{q} - \int_{\Omega \setminus (R \cup P)} \eta(\mathbf{q}) \mathcal{P}^b 1_{\bar{B}}(\mathbf{q}) e^{-\beta V(\mathbf{q})} d\mathbf{q} \\ &= \int_{\Omega \setminus (\bar{A} \cup \bar{B})} \eta(\mathbf{q}) [(I - \mathcal{P}^i) p^*(\mathbf{q}) - \mathcal{P}^b 1_{\bar{B}}(\mathbf{q})] e^{-\beta V(\mathbf{q})} d\mathbf{q}. \end{aligned}$$

The second equality holds as  $\mathcal{P}^i$  is self adjoint on  $L^2_\mu(\Omega \setminus (\bar{A} \cup \bar{B}))^{18}$

<sup>18</sup>Li, Khoo, Ren, Ying, In Proceedings of the 2nd Mathematical and Scientific Machine Learning Conference, Vol. 145, 2022

- Sebastian Barschkis. Exact and soft boundary conditions in physics-informed neural networks for the variable coefficient poisson equation, 2023. URL <https://arxiv.org/abs/2310.02548>.
- Charles-Edouard Bréhier, Tony Lelièvre, and Mathias Rousset. Analysis of adaptive multilevel splitting algorithms in an idealized case. *ESAIM - Probab. Stat.*, 19:361–394, 2015. doi: 10.1051/ps/2014029.
- Haochuan Chen, Benoît Roux, and Christophe Chipot. Discovering reaction pathways, slow variables, and committor probabilities with machine learning. *Journal of Chemical Theory and Computation*, 19(14):4414–4426, 2023. doi: 10.1021/acs.jctc.3c00028. URL <https://doi.org/10.1021/acs.jctc.3c00028>. PMID: 37224455.
- Frédéric Cérou and Arnaud Guyader. Adaptive multilevel splitting for rare event analysis. *Stochastic Analysis and Applications*, 25(2):417–443, feb 2007. doi: 10.1080/07362990601139628.
- M. Frassek, A. Arjun, and P. G. Bolhuis. An extended autoencoder model for reaction coordinate discovery in rare event molecular dynamics datasets. *The Journal of Chemical Physics*, 155(6):064103, aug 2021. doi: 10.1063/5.0058639.
- Ziwei He, Christophe Chipot, and Benoît Roux. Committor-consistent variational string method. *The Journal of Physical Chemistry Letters*, 13(40):9263–9271, sep 2022. doi: 10.1021/acs.jpcllett.2c02529.
- Hendrik Jung, Roberto Covino, A Arjun, Christian Leitold, Christoph Dellago, Peter G Bolhuis, and Gerhard Hummer. Machine-guided path sampling to discover mechanisms of molecular self-organization. *Nat. Comput. Sci.*, 3(4):334–345, April 2023.

- Peilin Kang, Enrico Trizio, and Michele Parrinello. Computing the committor with the committor to study the transition state ensemble. *Nat. Comput. Sci.*, 4(6):451–460, June 2024.
- Yuehaw Khoo, Jianfeng Lu, and Lexing Ying. Solving for high-dimensional committor functions using artificial neural networks. *Research in the Mathematical Sciences*, 6(1), oct 2018. doi: 10.1007/s40687-018-0160-2.
- Haoya Li, Yuehaw Khoo, Yinuo Ren, and Lexing Ying. A semigroup method for high dimensional committor functions based on neural network. In Joan Bruna, Jan Hesthaven, and Lenka Zdeborova, editors, *Proceedings of the 2nd Mathematical and Scientific Machine Learning Conference*, volume 145 of *Proceedings of Machine Learning Research*, pages 598–618. PMLR, 16–19 Aug 2022. URL <https://proceedings.mlr.press/v145/li22a.html>.
- Qianxiao Li, Bo Lin, and Weiqing Ren. Computing committor functions for the study of rare events using deep learning. *The Journal of Chemical Physics*, 151(5):054112, aug 2019. doi: 10.1063/1.5110439.
- Laura J. S. Lopes and Tony Lelièvre. Analysis of the adaptive multilevel splitting method on the isomerization of alanine dipeptide. *Journal of Computational Chemistry*, 40(11):1198–1208, jan 2019. doi: 10.1002/jcc.25778.
- Andrew R. Mitchell and Grant M. Rotskoff. Committor guided estimates of molecular transition rates. *Journal of Chemical Theory and Computation*, 20(21):9378–9393, 2024. doi: 10.1021/acs.jctc.4c00997. URL <https://doi.org/10.1021/acs.jctc.4c00997>. PMID: 39420582.

- Klaus Müller and Leo D. Brown. Location of saddle points and minimum energy paths by a constrained simplex optimization procedure. *Theoretica chimica acta*, 53:75–93, 1979.
- Maziar Raissi, Paris Perdikaris, and George Em Karniadakis. Physics informed deep learning (part i): Data-driven solutions of nonlinear partial differential equations, 2017. URL <https://arxiv.org/abs/1711.10561>.
- Grant M. Rotskoff and Eric Vanden-Eijnden. Learning with rare data: Using active importance sampling to optimize objectives dominated by rare events, 2020.
- Grant M Rotskoff, Andrew R Mitchell, and Eric Vanden-Eijnden. Active importance sampling for variational objectives dominated by rare events: Consequences for optimization and generalization. In Joan Bruna, Jan Hesthaven, and Lenka Zdeborova, editors, *Proceedings of the 2nd Mathematical and Scientific Machine Learning Conference*, volume 145 of *Proceedings of Machine Learning Research*, pages 757–780. PMLR, 16–19 Aug 2022. URL <https://proceedings.mlr.press/v145/rotskoff22a.html>.
- Benoît Roux. String method with swarms-of-trajectories, mean drifts, lag time, and committor. *The Journal of Physical Chemistry A*, 125(34):7558–7571, aug 2021. doi: 10.1021/acs.jpca.1c04110.
- Benoît Roux. Transition rate theory, spectral analysis, and reactive paths. *The Journal of Chemical Physics*, 156(13):134111, 04 2022. ISSN 0021-9606. doi: 10.1063/5.0084209. URL <https://doi.org/10.1063/5.0084209>.
- John Strahan, Justin Finkel, Aaron R. Dinner, and Jonathan Weare. Predicting rare events using neural networks and short-trajectory data. *Journal of Computational Physics*, 488:112152, 2023. ISSN 0021-9606. URL <https://doi.org/10.1016/j.jcp.2023.112152>.

0021-9991. doi: <https://doi.org/10.1016/j.jcp.2023.112152>. URL

<https://www.sciencedirect.com/science/article/pii/S0021999123002474>.

Yueyang Wang, Kejun Tang, Xili Wang, Xiaoliang Wan, Weiqing Ren, and Chao Yang. Estimating committor functions via deep adaptive sampling on rare transition paths, 2025. URL  
<https://arxiv.org/abs/2501.15522>.

Jixin Yuan, Amar Shah, Channing Bentz, and Maria Cameron. Optimal control for sampling the transition path process and estimating rates, 2023. URL <https://arxiv.org/abs/2305.17112>.